

On the error sensitivity of the GPS ambiguity success rate

P. Joosten and P.J.G. Teunissen
Department of Mathematical Geodesy and Positioning
Delft University of Technology
Thijssseweg 11
2629 JA Delft, The Netherlands
Fax: ++ 31 15 278 3711
Email: P.Joosten@geo.tudelft.nl

BIOGRAPHY

Dr. Peter Teunissen is Professor of Mathematical Geodesy and Positioning. Peter Joosten graduated at the Faculty of Geodesy of the Delft University of Technology. They are currently engaged in the development of GPS data processing strategies for medium scaled networks with an emphasis on ambiguity resolution.

ABSTRACT

GPS ambiguity resolution is the process of resolving the unknown cycle ambiguities of the double-difference (DD) carrier phase data as integers. It is the key to high-precision relative GPS positioning, when only short observation time spans are used. Once the integer ambiguities are resolved, the carrier phase measurements will start to act as if they were high-precision pseudo range measurements, thereby allowing the remaining parameters, such as the baseline coordinates, to be estimated with a comparable high precision. High ambiguity success rates are required for GPS ambiguity resolution to be successful. These success rates, as measured by the probabilities of correct integer estimation, depend on the various assumptions underlying the mathematical model used. Mis-specifications or errors in either the functional or stochastic model will generally result in lower success rates. It is therefore of importance to be able to diagnose the sensitivity of ambiguity resolution for such type of errors.

In this contribution we will analyse the sensitivity of GPS ambiguity resolution for various type of modeling errors. The analysis is based on an analytical, closed form formula for the probability of correct integer estimation. This formula is generally valid and may be applied to any of the GPS models currently in use. In the present contribution it will be used to study the error sensitivity of the GPS geometry-free model.

INTRODUCTION

Ambiguity resolution is the key to fast and high-precision relative positioning, both in the case of current GPS and future GNSS's. The reason for this is that once the ambiguities have been resolved as integers, the phase measurements start to act as if they were high-precision range

measurements, thereby allowing the parameters of interest (e.g. baseline-coordinates) to be estimated with a comparable high precision. Ambiguity resolution applies to a great variety of GPS models currently in use. They range from single-baseline models for kinematic positioning to multi-baseline models used as a tool for studying geodynamical phenomena. Models may have the relative satellite-receiver geometry included or excluded. Receivers may be stationary or in motion. Atmospheric delays may be included in the model as unknowns, making the model suitable for long baselines, or they may be excluded from the model, making the model suitable for relatively short baselines. An overview of these possible models, as well as their applications, can be found in a number of textbooks like Hofmann-Wellenhof *et al.* (1997), Leick (1995), Parkinson and Spilker (1996), Strang and Borre (1997) and Teunissen and Kleusberg (1998).

For all these different models, the method of ambiguity resolution is the same, and usually a three-step procedure is followed. In a first step, the integer character of the ambiguities is discarded, and a standard least-squares adjustment is carried out. This provides us with real-valued estimates for the unknown parameters, often referred to as the "float solution". This step also provides us with the variance-covariance matrix of these unknowns. In a second step, the float ambiguity estimates are used to compute the corresponding integer ambiguity estimates, the actual ambiguity resolution step. Finally, providing the second step was successful, this integer estimate is used to correct the float solution estimate. As a result one obtains the final and precise estimates for the remaining parameters of interest, usually, but not necessarily, baseline-coordinates.

The integer estimation part of this three-step procedure essentially boils down to applying a mapping function from the n -dimensional space of real values to the n -dimensional space of integer values. Several possibilities are available here, such as a simple rounding of the ambiguities, a conditional rounding of the ambiguities (bootstrapping), or an integer least-squares mapping of the ambiguities. These possibilities differ in complexity, but more important, they differ in the probability of estimating the *correct* integers. It has been proven in Teunissen (1999) that the integer least-squares estimator is

optimal in the sense that it maximizes the probability of correct integer ambiguity estimation. This integer least-squares estimator is also the most complex of the estimators mentioned, but it has been efficiently mechanized in the LAMBDA-method which was introduced in Teunissen (1993).

The probability of successful ambiguity resolution, also referred to as the success rate of ambiguity resolution, is given as the integral:

$$P(\tilde{a} = a) = \int_{S_a} p_{\hat{a}}(x) dx \quad (1)$$

with $p_{\hat{a}}(x)$ the probability density function of the float ambiguities and S_a the pull-in region. It is stressed that the success rate should be used as measure for predicting the success of ambiguity resolution instead of e.g. the standard deviations of the ambiguities.

Note that the success rate depends on three factors, being the functional model (observation equations), the stochastic model (distribution and precision of the observables) and the chosen method of integer estimation.

The unbiasedness of the 'float' solution is one of the basic assumptions underlying the computation of the ambiguity success rate. This assumption is valid as long as the 'float' solution is based on a correctly specified model. Any mis-specification in the functional model (the observation equations) however, will generally lead to biases in the least-squares estimator and therefore in the 'float' solution of the ambiguities. In case of GPS, such biases could be generated by outliers in the code data, cycle slips in the phase data, multipath or the presence of unaccounted atmospheric delays. In this contribution we will discuss the impact such biases have on the performance of ambiguity resolution.

THE INFLUENCE OF BIASES ON THE SUCCESS RATE

A one-dimensional example

Since unaccounted biases will degrade the performance of ambiguity resolution, the ambiguity success rate will get smaller in the presence of such biases. A smaller success rate, however, does not necessarily mean that it has become unacceptably small. It could still be large enough, even in the presence of biases. This is illustrated in figure 1 for a one-dimensional example. In this figure, the success rate equals the integral of the pdf of \hat{a} over the pull-in region, in this 1D-case the line-segment between -0.5 and 0.5 . In the absence of any bias, the pdf of \hat{a} will be centered at a . Thus, the success rate in the unbiased case equals the blue area in the figure on top. But when a bias b is present it will translate over b and be centered at $a + b$. The success rate still equals the integral of the pdf of \hat{a} over the pull-in region, in this case the red area. Since the red area is smaller than the blue area, the translation over b will reduce the success rate.

However, if the pdf were sufficiently peaked, as shown in

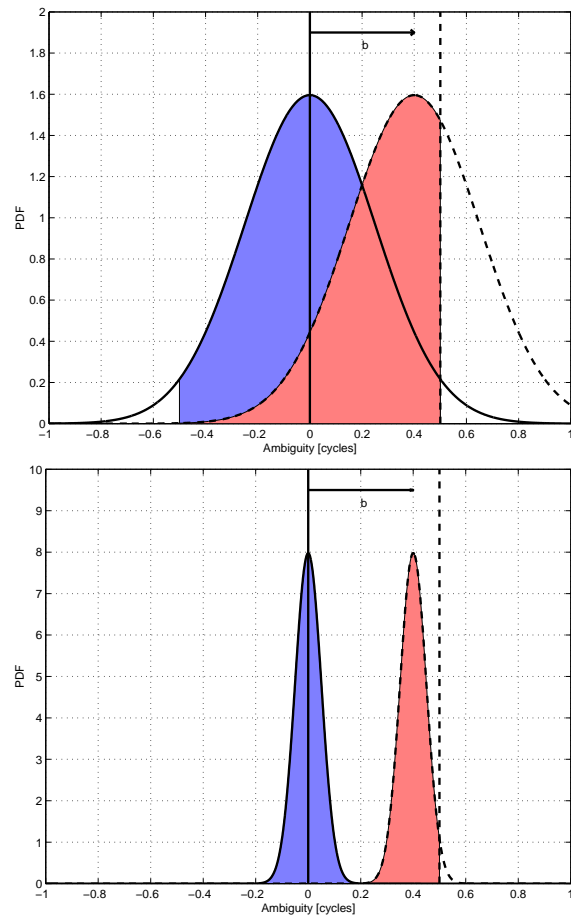


Fig. 1. One-dimensional example of the effect of a bias in the float ambiguity on the success rate, on top the standard deviation of the ambiguity is chosen to be 0.25 cycle, at the bottom it is chosen as 0.05 cycle.

figure 1 at the bottom, the success rate could still be large enough, even though the pdf is now centered at $a + b$. In fact, if the pdf were sufficiently peaked, the success rate would not change by much, provided the vector $a + b$ remains located within the pull-in region. A dramatic drop in the success rate's value will then only occur when $a + b$ crosses the boundary of the pull-in region.

In order to gain some understanding for the relationship that exists between precision of the float ambiguity, bias and success rate, figure 2 has been provided. This figure shows that biases less than 0.5 cycle are permitted, provided the corresponding standard deviation is small enough. That is, provided the distribution is sufficiently peaked. The high success rate drops dramatically though when the limit of a 0.5 cycle is crossed.

A general formula

In this section we present an exact and easy-to-compute formula for the bootstrapped success rate in the presence of bias. This general formula can be used to evaluate the influence of biases on the bootstrapped success rate. Inte-

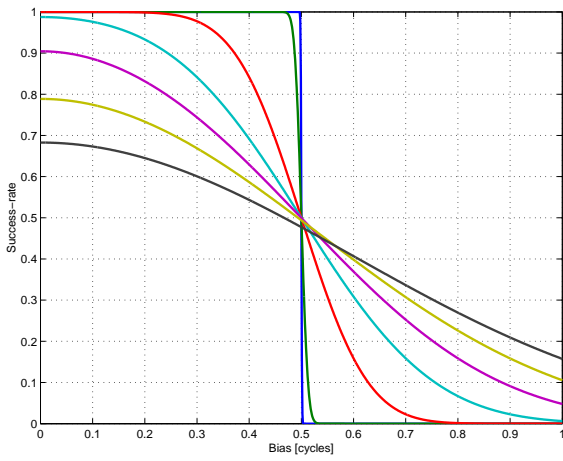


Fig. 2. Success rates as function of the bias b . The seven success rate curves correspond with $\sigma_{\hat{a}} = 0.001, 0.01, 0.1, 0.2, 0.3, 0.4, 0.5$ cycles.

ger bootstrapping is an often used method of integer ambiguity estimation. It is a simple method, which, when combined with the decorrelation process of the LAMBDA method, can achieve good results. The method is a generalization of the 'integer rounding' method and goes as follows. If n ambiguities are available, one starts with the first ambiguity \hat{a}_1 and rounds its value to the nearest integer. Having obtained the integer value of this first ambiguity, the real-valued estimates of all remaining ambiguities are then corrected by virtue of their correlation with the first ambiguity. Then the second, but now corrected, real-valued ambiguity estimate is rounded to its nearest integer. Having obtained the integer value of the second ambiguity, the real-valued estimates of all remaining $n - 2$ ambiguities are then again corrected, but now by virtue of their correlation with the second ambiguity. This process is continued until all ambiguities are taken care of. In essence this 'bootstrapping' technique boils down to the use of a sequential conditional least-squares adjustment, with a conditioning on the integer ambiguity values obtained in the previous steps.

The method of integer bootstrapping is known to perform poorly when it is applied to the double-difference (DD) ambiguities. This is due to the usually high correlation between the DD ambiguities. The method should therefore only be applied to ambiguities which are sufficiently decorrelated. This is achieved by applying the decorrelating Z-transformation of the LAMBDA method, see Teunissen (1993), de Jonge and Tiberius (1996). Hence, instead of applying integer bootstrapping to the DD ambiguity vector \hat{a} , it should be applied to the transformed and decorrelated ambiguities,

When the original DD ambiguities are biased, the transformed ambiguities will be biased too. They are distributed as

$$\hat{z} \sim N(z + Z^T b, Q_z = Z^T Q_{\hat{a}} Z) \quad (2)$$

with z the true, but unknown transformed integer ambiguity vector and $Z^T b$ the transformed bias vector. We are now in the position to describe how the bootstrapped success rate is affected by the presence of biases.

Theorem Let the real-valued 'float' solution be biased and distributed as in (2) and let the integer solution be obtained by means of bootstrapping. The probability of correct integer bootstrapping is then given as

$$P_b(\hat{a} = z) = \prod_{i=1}^n \left[\Phi \left(\frac{1 - 2\zeta_i}{2\sigma_{\hat{z}_{i|l}}} \right) + \Phi \left(\frac{1 + 2\zeta_i}{2\sigma_{\hat{z}_{i|l}}} \right) - 1 \right] \quad (3)$$

with ζ_i the i^{th} entry of the bias vector $L^{-1}Z^T b$, $\sigma_{\hat{z}_{i|l}}$ the variance of the i^{th} least-squares ambiguity obtained through a conditioning on the previous $l = 1, \dots, (i - 1)$ ambiguities and

$$\Phi(x) = \int_{-\infty}^x \frac{1}{\sqrt{2\pi}} \exp\left\{-\frac{1}{2}v^2\right\} dv \quad (4)$$

The lower unit triangular matrix L follows from the factorization $Q_z = LDL^T$, while $D = \text{diag}(\dots, \sigma_{\hat{z}_{i|l}}^2, \dots)$.

This theorem was first introduced and proved in Teunissen *et al.* (2001). In the next section we will use the above theorem to study the impact biases have on the ambiguity success rate of the geometry-free model.

THE GEOMETRY-FREE GPS MODEL

The float ambiguity solution

For sufficiently short baselines, the DD phase and code observation equations of the dual frequency, geometry-free GPS model are given for a single epoch i as:

$$\begin{aligned} \phi_1(i) &= \rho(i) + \lambda_1 a_1 \\ \phi_2(i) &= \rho(i) + \lambda_2 a_2 \\ p_1(i) &= \rho(i) \\ p_2(i) &= \rho(i) \end{aligned} \quad (5)$$

where $\phi_1(i)$ and $\phi_2(i)$ are the DD phase observables on L1 (1575.420 MHz) and L2 (1227.600 MHz). $p_1(i)$ and $p_2(i)$ are the corresponding DD code observables, $\rho(i)$ is the DD form of the unknown receiver-satellite range and a_1 and a_2 are the unknown but time-invariant integer DD ambiguities. The known wavelengths are denoted as λ_1 and λ_2 .

Note, due to the parametrization in terms of the DD ranges, that no linearization is required for the above observation equations. The absence of the receiver-satellite geometry also implies that the model permits both receivers to be either stationary or moving. Furthermore, the parametrization in terms of the DD ranges implies that the tropospheric delays need not be modelled explicitly. When present, these delays will get lumped with the DD ranges. Hence the estimated ambiguities will always be free from tropospheric biases.

The geometry-free GPS model has been studied by many, see e.g. Euler and Goad (1990), Hatch (1982), Jonkman (1998), Joosten *et al.* (1999), Teunissen (1996), Wübbena (1988).

In the following it will be assumed that the 'float' solution of the above model is obtained in a least-squares sense using k number of epochs. The ambiguities are considered to be time-invariant for the duration of the observation period. We also assume that time correlation and cross correlation are absent. The undifferenced standard deviations of phase and code will be denoted as σ_ϕ and σ_p respectively. Once the 'float' solution of the ambiguities is obtained, the integer bootstrapping principle can be applied and the corresponding probability of correct integer estimation can be computed.

The DD float solution of the above model can be shown to read as:

$$\begin{cases} \hat{a}_1 &= \frac{1}{k\lambda_1} \sum_{i=1}^k \{\phi_1(i) - \frac{1}{2}(p_1(i) + p_2(i))\} \\ \hat{a}_2 &= \frac{1}{k\lambda_2} \sum_{i=1}^k \{\phi_2(i) - \frac{1}{2}(p_1(i) + p_2(i))\} \end{cases} \quad (6)$$

We are therefore now in the position to formulate the effect various biases have on the float solution. This result combined with the above given theorem, enables one to evaluate the bias affected success rate.

Outliers in the code data

An outlier (blunder) in the L1 code data at epoch j ($1 \leq j \leq k$) of size ∇_{p_1} , will produce a bias in the float ambiguity vector of

$$b = -\frac{1}{2k} \begin{bmatrix} \frac{\nabla_{p_1}}{\lambda_1} \\ \frac{\nabla_{p_1}}{\lambda_2} \end{bmatrix} \quad (7)$$

Figure 3 shows the dual frequency success rate as a function of the size of the code outlier, ∇_{p_1} , for $k = 1, 5$ and 10 , with $\sigma_\phi = 3\text{mm}$ and $\sigma_p = 10\text{cm}$.

These results may come as a surprise, since they show that successful ambiguity resolution is quite insensitive to the presence of a code outlier of moderate size. For instance, for $k=5$, the success rate is still close to 1 even in the presence of a code outlier of 3 m. The results shown can be explained as follows. The success rate's insensitivity is caused by two effects, the length of the b vector as governed by k and the direction of the b vector. The direction of b is favourable since it can be shown to point in the most elongated direction of the DD pull-in region. But also the effect of a larger value for k is favourable, since when k increases, the length of b decreases, and the pdf of \hat{a} gets more peaked, while the pull-in region remains unaffected.

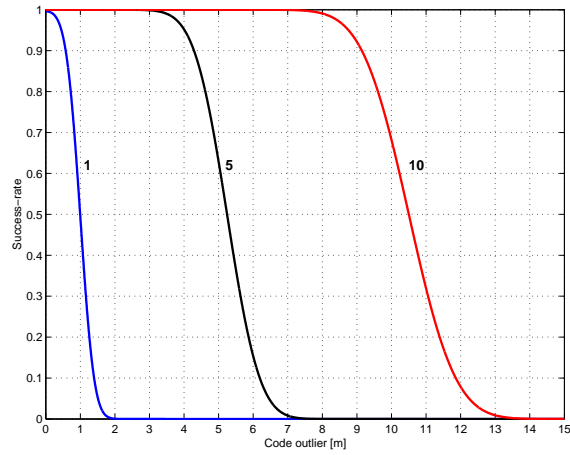


Fig. 3. Dual frequency success rate as a function of the size of the code outlier, ∇_{p_1} (m), for $k = 1$ (blue), 5 (black), and 10 (red), with $\sigma_\phi = 3\text{mm}$ and $\sigma_p = 10\text{cm}$.

Slips in the phase data

A slip in the L1 phase data at epoch j ($1 \leq j \leq k$) of size ∇_{ϕ_1} (cycle), will produce a bias in the float ambiguity vector of

$$b = -\frac{k-j+1}{k} \nabla_{\phi_1} \begin{bmatrix} 1 \\ 0 \end{bmatrix} \quad (8)$$

Figure 4 shows the dual frequency success rate as a function of the size of the phase slip, ∇_{ϕ_1} , for $k = 1, 5$ and 10 , with $\sigma_\phi = 3\text{mm}$ and $\sigma_p = 10\text{cm}$. For the start of the slip, three different cases are evaluated: first epoch ($j = 1$), halfway time interval ($j = \frac{k+1}{2}$ when $k = \text{odd}$, $j = \frac{k}{2}$ otherwise) and last epoch ($j = k$).

The results show that the permitted size of the slip depends very much on the moment the slip started to occur. In particular when this moment comes close to the last epoch, much larger slips are permitted, in case of $k=10$ even larger than 1 cycle. When $j = k$, the success rate's dependence on the size of the slip is very similar to what we saw in case of the code-outlier.

Effect of unaccounted ionospheric delays

It is common practice to neglect the ionospheric delays in case of sufficiently short baselines. The model in which the ionospheric delays are assumed known or absent is referred to as the ionosphere-fixed model, and is given in (5). But when are we truly allowed to use this simplified model? That is, when do baselines satisfy the criterion of 'sufficiently short'? This is usually determined on the basis of experiments and past experience. With the above given theorem however, we now have an additional tool for studying the impact of ionospheric biases. Furthermore, such studies are now easily performed for various measurement scenarios. In the following we will study the impact of the ionospheric biases for the the dual- and the triple-frequency case and compare the

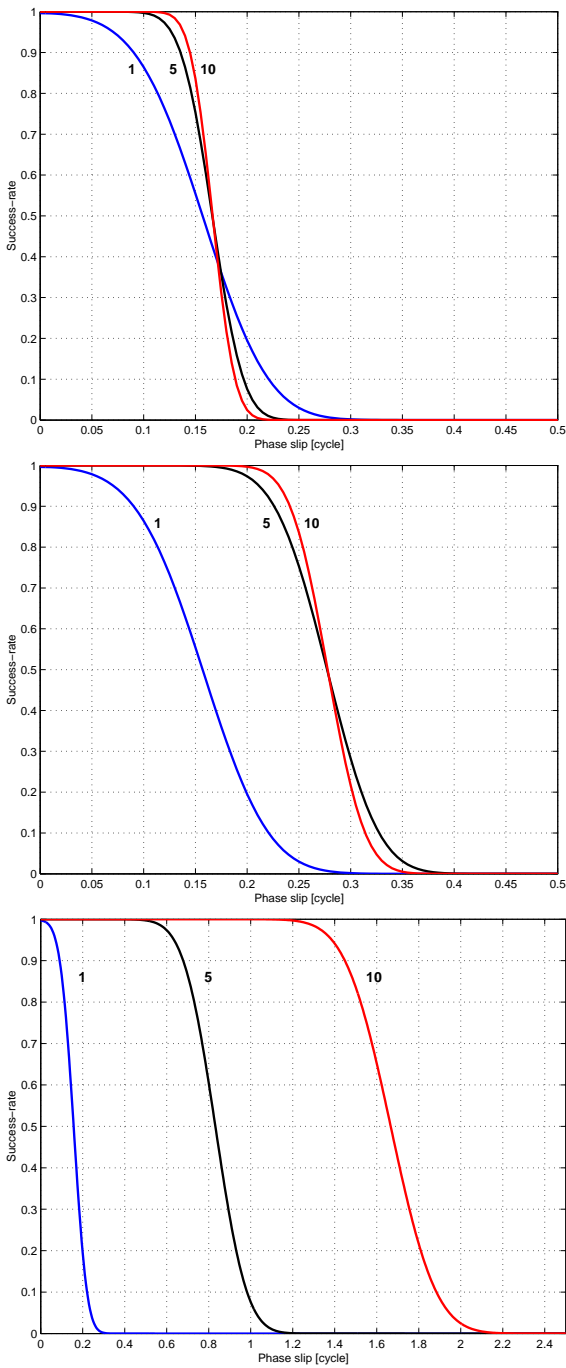


Fig. 4. Dual frequency success rate as a function of the size of the phase slip, $\nabla\phi_i$, for $k = 1$ (blue), 5 (black), and 10 (red), with $\sigma_\phi = 3\text{mm}$ and $\sigma_p = 10\text{cm}$. On top, the slip occurs at the first epoch, in the middle halfway the interval, and at the bottom at the last epoch.

performance of the bias affected, ionosphere-fixed model with the performance of its most relaxed alternative, the ionosphere-float model.

The ionospheric biases can be shown to affect the

ionosphere-fixed, float ambiguity solution as:

$$b = \tau \begin{bmatrix} 2\lambda_1 + \frac{1}{2}\lambda_1 \left(\frac{\lambda_2^2}{\lambda_1^2} - 1 \right) \\ 2\lambda_2 + \frac{1}{2}\lambda_2 \left(\frac{\lambda_1^2}{\lambda_2^2} - 1 \right) \end{bmatrix} \quad (9)$$

$$\text{with } \tau = \frac{40.3}{c^2} 10^{16} \overline{TECU} (m^{-1}),$$

$$\overline{TECU} = \frac{1}{k} \sum_{i=1}^k TECU(i)$$

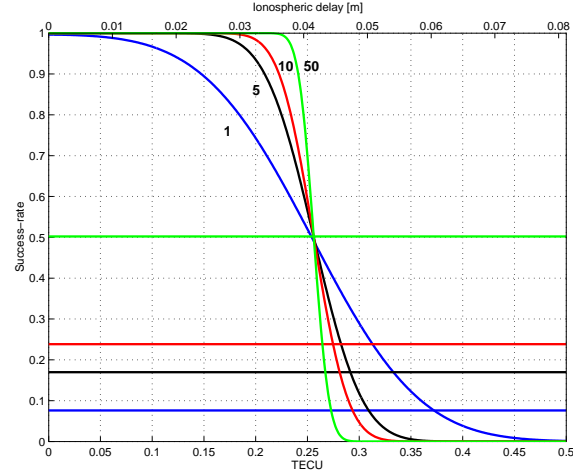


Fig. 5. Success rates as a function of bias due to unmodeled ionospheric delays for a number of epochs of 1, 5, 10 and 50, with $\sigma_\phi = 3\text{mm}$, $\sigma_p = 10\text{cm}$. Success rates based on the ionosphere-float model for the same number of epochs are shown as horizontal lines.

Figure 5 shows the dual frequency success rate as a function of \overline{TECU} , for $k = 1, 5, 10$ and 50, with $\sigma_\phi = 3\text{mm}$ and $\sigma_p = 10\text{cm}$.

The S-curves are the success rates based on the ionosphere-fixed model, and the horizontal lines are the success rates based on the ionosphere-float model. It is well-known that the dual-frequency, ionosphere-fixed, geometry-free model permits fast ambiguity resolution in the absence of ionospheric biases. This is also shown in figure 5. However, since one can never be sure, even for short baselines, whether the ionospheric delays are truly absent, it is of interest to know how sensitive the success rate is for the presence of such biases. From figure 5 we learn that the single-epoch success rate drops to about 80% in case the bias equals about 3 cm. This shows that already a few centimeters of an ionospheric delay can lower the success rate significantly. Hence, if one wants to safeguard ambiguity resolution against the presence of such biases one should take more epochs into account. For the present example ten epochs instead of one would suffice. Fortunately the presence of such biases does not yet necessitate the use of the ionosphere-float model. This would be the case when the biases become larger. But then the success rates become so small, that fast, full ambiguity resolution will not be possible anymore. In that case partial ambiguity resolution might be an alternative.

Note that, although the permitted biases are small, they are time-averaged, double-differenced biases and not absolute ionospheric biases.

Sensitivity in case of partial ambiguity resolution

For full ambiguity resolution we have seen, in case the double-differenced, time-averaged ionospheric delay amounts to only a few centimeters, that the ionosphere-fixed model is to be preferred over the ionosphere-float model. Although the latter model permits ionospheric delays of any size, too many epochs are needed with this model to reach a sufficiently high success rate. With the ionosphere-fixed model, on the other hand, one can still reach a high success rate reasonably fast, provided the ionospheric bias is less than a few centimeters.

As an alternative to full ambiguity resolution, one may consider partial ambiguity resolution. With a dual-frequency model, partial ambiguity resolution amounts to fixing the best determined ambiguity, whereas with a triple-frequency model, it amounts to a fixing of the two best determined ambiguities. The selection of the best determined ambiguities is based on the LAMBDA method.

Partial ambiguity resolution is attractive in case full ambiguity resolution would take too many epochs to reach a sufficiently high success rate. As shown in Teunissen *et al.* (1999), fast partial ambiguity resolution is possible with the ionosphere-float model. Although the precision improvement in the range ρ is less with partial ambiguity resolution than it would have been with full ambiguity resolution, the improvement is still significant.

The question arises now whether one can speed up partial ambiguity resolution even further by applying it to the bias affected, ionosphere-fixed model, instead of to the ionosphere-float model. It turns out that this is only possible in case the precision of the code data is relatively poor. Table 1 shows the results for modernised three-frequency GPS based on a code precision of 30 cm.

Success rate	Number of epochs necessary					
	float	Ionosphere fixed, bias \leq [cm]				
		10	20	30	40	50
0.9900	5	2	2	2	3	4
0.9950	6	2	2	3	3	4
0.9990	9	3	3	4	4	6
0.9999	12	4	4	5	7	9

Table 1. Number of epochs needed, in case of modernised GPS, for the ionosphere-float model and the bias affected, ionosphere-fixed model, to reach a certain partial ambiguity success rate (99%, 99.5%, 99.9%, 99.99%). Five levels (10-50cm) are shown for the maximum allowable ionospheric bias in case the ionosphere-fixed model is used. The chosen precision of phase and code reads $\sigma_\phi = 3\text{mm}$ and $\sigma_p = 30\text{cm}$.

Table 1 shows, for instance, if a success rate of 99.99% is required, that 12 epochs would be needed with the ionosphere-float model, but only 4 epochs with the ionosphere-fixed model, provided the ionospheric bias is less than 20 cm. In case of 12 epochs the precision of the DD range improves from 44 cm (ambiguities floated) to 17 cm (two best determined ambiguities fixed), whereas with 4 epochs it improves from 76 cm to 29 cm.

References

- de Jonge, P. and Tiberius, C. (1996). The LAMBDA method for integer ambiguity estimation: implementation aspects. Technical Report LGR Series, No. 12, Delft Geodetic Computing Centre, Delft University of Technology, The Netherlands.
- Euler, H. and Goad, C. (1990). On optimal filtering of GPS dual-frequency observations without using orbit information. *Bulletin Geodesique*, **65**, 130–143.
- Hatch, R. (1982). The synergism of GPS code and carrier-phase measurements. In *Proceedings 3rd International Geodetic Symposium on Satellite Positioning*, volume 2, pages 1213–1231.
- Hofmann-Wellenhof, B., Lichtenegger, H., and Collins, J. (1997). *Global Positioning System: Theory and Practice*. Springer Verlag, Berlin, fourth edition.
- Jonkman, N. (1998). The geometry-free approach to integer gps ambiguity estimation. In *Proceedings of ION GPS-98, Nashville, TN, September 15-18*, pages 369–379.
- Joosten, P., Teunissen, P., and Jonkman, N. (1999). Gns three carrier phase ambiguity resolution using the LAMBDA method. In *Proceedings GNSS'99, 3rd European Symposium on Global Navigation Satellite Systems, 5-8 October, Genova, Italy*, pages 367–372.
- Leick, A. (1995). *GPS Satellite Surveying*. John Wiley and Sons, New York, second edition.
- Parkinson, B. and Spilker, J., editors (1996). *GPS: Theory and Applications*. AIAA, Washington DC.
- Strang, G. and Borre, K. (1997). *Linear Algebra, Geodesy, and, GPS*. Wellesley-Cambridge Press.
- Teunissen, P. (1993). Least-squares estimation of the integer GPS ambiguities. In *IAG General Meeting, Invited Lecture, Section IV Theory and Methodology, Beijing, China*.
- Teunissen, P. (1996). An analytical study of ambiguity decorrelation using dual frequency code and carrier phase. *Journal of Geodesy*, **70**(8), 515–528.
- Teunissen, P. (1999). A theorem on maximizing the probability of correct integer estimation. *Artificial Satellites*, **34** (1), 3–9.
- Teunissen, P. and Kleusberg, A., editors (1998). *GPS for Geodesy*. Springer Verlag, Berlin, second enlarged edition.
- Teunissen, P., Joosten, P., and Tiberius, C. (1999). Geometry-free ambiguity success rates in case of partial fixing. In *Proceedings ION GPS NTM99*, pages 201–210.
- Teunissen, P., Joosten, P., and Tiberius, C. (2001). Bias robustness of GPS ambiguity resolution. In *Proceedings ION GPS-2000*.
- Wübbena, G. (1988). GPS carrier phases and clock modelling. *GPS techniques applied to Geodesy and Surveying*. Groten, E. and R. Strauss (eds), *Lecture notes in Earth Sciences*, **19**, 381–392.